EAN 2017
55th conference on experimental stress analysis

Cyclic Tensile Tests of Epoxy Resin and the Experimentally Obtained Data Processing

Hana Srbová[1, a], Tomáš Kroupa[2, b]

[1, 2] University of West Bohemia, NTIS – New Technologies for the Information Society, Univerzitní 22, 306 14, Plzeň, Czech Republic, tel.: +420 377 63 2308

[a] hsrbova@kme.zcu.cz, [b] kroupa@kme.zcu.cz

Keywords: tensile test, data processing, loading cycle, envelope curve, damage factor, hardening curve

Material parameters of epoxy resin subjected to cyclic tensile tests are derived from the experimentally obtained data. The cyclic tensile tests are processed to obtain material parameters necessary to define a material model in a finite element software including damage and plastic behavior. A library of functions was written in programming language *Python* for purposes of the data processing.

Introduction

In order to examine mechanical response of one type of composite matrix, specimens made of epoxy resin were subjected to cyclic tensile loading with increasing amplitude. Low molecular weight epoxy resin CHS-EPOXY 520 was hardened with CHS-P 11 and cured in a shape of a plate at room temperature before cutting the specimens. The manufacturing process was performed according to standard test method ASTM D638-10 [1]. Three groups of specimens varied in the curing time, from one week to 9 months.

The paper includes description of obtaining the key information from the experimental data, their averaging and further data processing for the use in FE or semi-analytical isotropic elasto-plastic-damage material model. The data are processed with the aim to obtain quantities or information such as Young's modulus, hardening curve or dependency between damage factor and energy necessary to damage level increase.

Experiments

Specimens were manufactured according to standard test method ASTM D638-10 Tensile Properties of Plastics and divided into 3 groups according to their curing time:

1. 7 days
2. 152 days
3. 255 days

Both, the manufacturing and the curing process were performed at room temperature.

Tensile tests were performed on test machine ZWICK ROELL/Z050 with clip-on biaxial extensometer BTC-EXACLBI.001. Specimens were subjected to cyclic tensile loading with increasing amplitude until failure (Fig. 1). Unloading in each cycle started when gage area elongation exceeded a multiple of Δl = 0.02 mm. Loading in the corresponding cycle started when tensile force decreased under 30 % of force value at the start of the unloading.

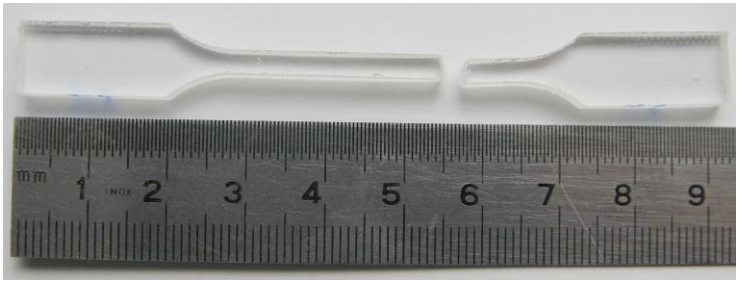

Figure 1: Cracked specimen.

Data Processing

Data from the experiments were further processed using *ploTRA* - library of functions developed for purposes of processing experimental data written in *Python* programming language. Loading force F, elongation Δl of gage area l_g = 25 mm and transverse strain of the specimen were recorded during the tests.

Engineering stress σ and strain ε were defined as

$$\sigma = \frac{F}{A_0} \qquad \text{and} \qquad \varepsilon = \frac{\Delta l}{l_g}. \tag{1}$$

The cross-section area A_0 change is neglected. In case of finite strain, true stress σ_{true} and strain ε_{true} would be considered.

Specific points of all loading cycles in shape of force-displacement dependency $F(\Delta l)$ and stress-strain dependency $\sigma(\varepsilon)$ (Fig. 2) were identified. The exact position of the intersection point P_{int} was found and maxima — P_{max} and minima — P_{min} of the loading cycles were defined. In case of stress-strain dependencies, all the points were identified in terms of strain ε and in case of force-displacement dependencies, the P_{min} points were identified in terms of displacement Δl and the P_{max} points in terms of force F. To obtain a representative behavior of all the specimens within the set of specimens with the same curing time, the specific points — P_{min}, P_{int} and P_{max} were averaged for each group of specimens in terms of both coordinates – stress–strain and force–displacement.

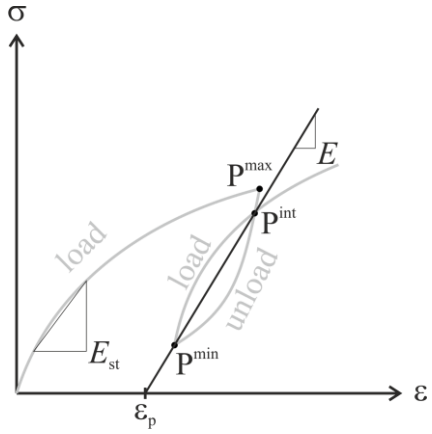

Figure 2: Loading cycle and specific points.

The averaged specific points were further used for definition of averaged envelope curve for each set of experiments and the tangents of the loading cycles. An envelope curve was set as the curve connecting points P_{max}. Tangents of the cycles, which can be considered as moduli E are identified as the slope of a line connecting given averaged cycle intersection point and minimum point (P_{int} and P_{min}). In general, Young's modulus is defined in standard

ČSN EN ISO 527-1 [2] from the difference between two strain points $\Delta\varepsilon$ (0.05% and 0.25%) and the difference in applied stress between the two strain points as $E_{st} = \Delta\sigma/\Delta\varepsilon$ (Fig. 2). It can be more convenient, however, to determine it as the slope of a linear regression line from the data points on the given strain interval. Values of the identified Young's moduli E_{st} and other parameters obtained from the averaged data are in Tab. 1. Plastic strain ε_p for reached strain ε given by the point P_{max} is obtained as the value of intersection of the line connecting P_{int} and P_{min} and the axis ε.

Table 1: Averaged data for sets of specimens obtained from experimental tests.

Curing time t [days]	Young's modulus E_{st} [MPa]	Max. stress σ_{max} [MPa]	Max. strain ε_{max} [%]	Achieved cycles
7	3.73	40.50	1.20	14
152	3.40	59.37	2.77	32
255	3.41	63.28	3.26	40

The envelope curves

$$\sigma = \sigma(\varepsilon) \tag{2}$$

for the sets of experiments and the slopes of averaged loading cycles are shown in Fig. 3. The curves were resampled and point [ε, σ] = [0, 0] for the unloaded state was added. Values of strain ε, where the maximum stress σ_{max} was reached is different for engineering stress σ and for effective stress $\bar{\sigma}$, which is the stress in the undamaged part of the cross-section.

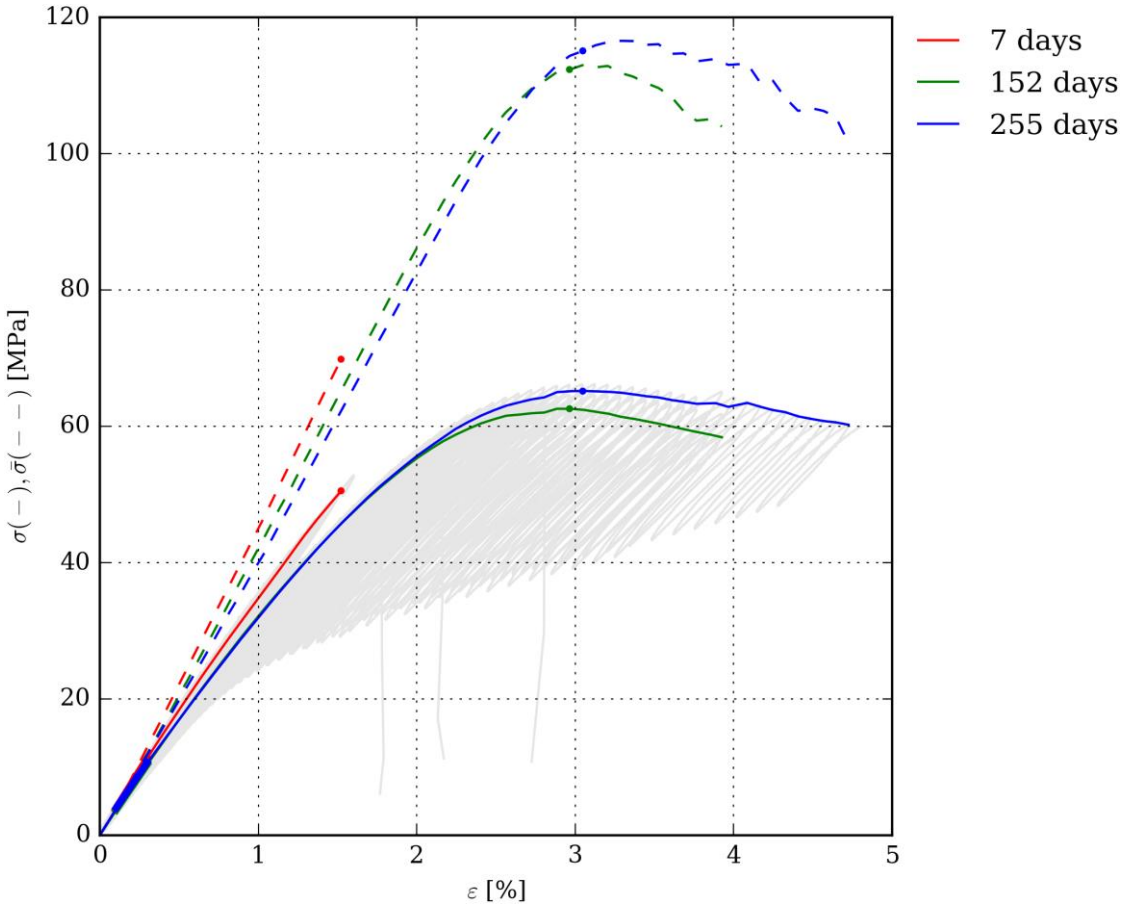

Figure 3: Envelope curves for sets of specimens, points of the highest reached stress σ_{max}, effective stress-strain dependencies.

Effective stress depicted in Fig. 3 was obtained as

$$\bar{\sigma}(\varepsilon) = \frac{\sigma(\varepsilon)}{1-D(\varepsilon)}, \tag{3}$$

where D is damage factor defined as

$$D(\varepsilon) = 1 - \frac{E(\varepsilon)}{E(0)}, \tag{4}$$

and $E(\varepsilon)$ is modulus of the loading cycle for strain ε defined at the P_{max} point and $E(0)$ is initial modulus. It is the coordinate of point $[\varepsilon, E] = [0, E(0)]$ of a line connecting the first two moduli (moduli of the first two cycles) of modulus-strain dependency (Fig. 4).

$$E = E(\varepsilon). \tag{5}$$

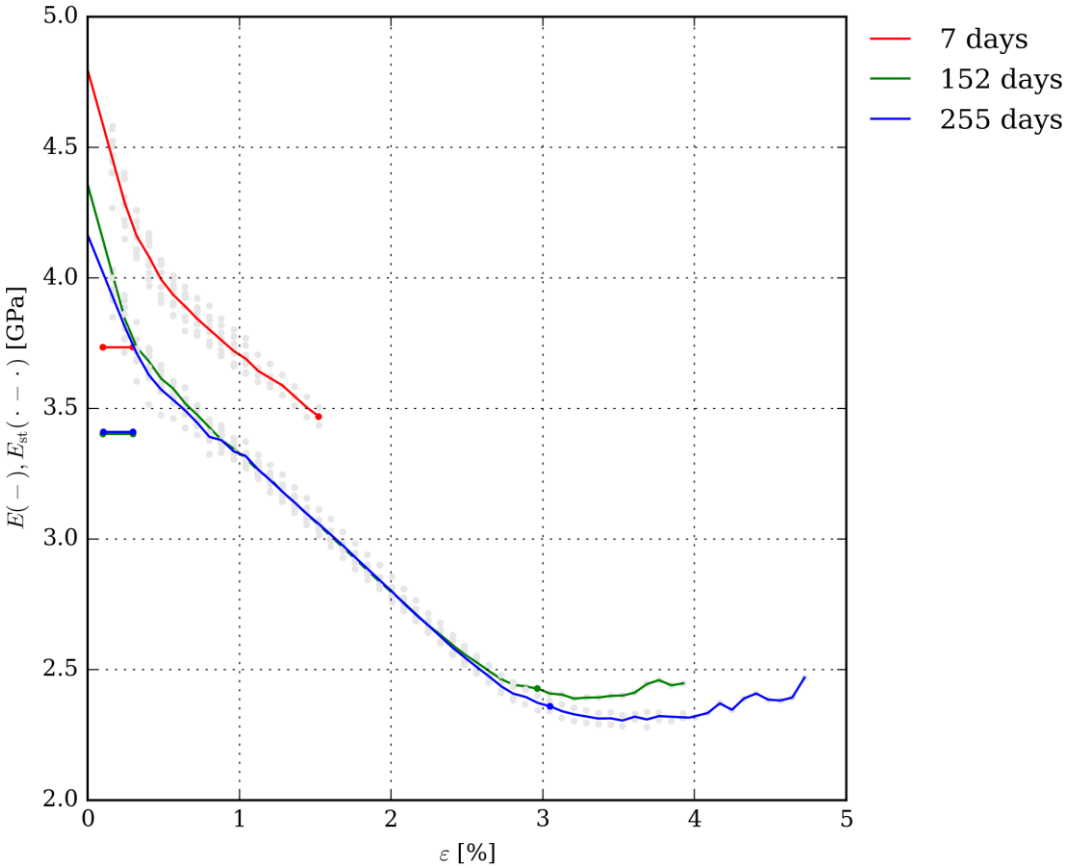

Figure 4: Modulus-strain dependencies, Young's moduli E_{st} depicted on the strain interval defined in standard, and points of the highest reached stress.

The epoxy resin showed damage behavior, since the values of the cycle moduli E are a decreasing function of the maximum reached strain ε. In case of the specimens cured for 152 and 255 days, the values of the cycle tangents slightly increased just before failure. It is caused by the definition of loading cycles leading to incorrect values for the advanced cycles. The material cured for 7 days has the highest stiffness, since the moduli of cycles E as well as the Young's modulus E_{st} = 3.7 GPa identified according to standard are the highest.

The material also showed plastic behavior. Dependency of plastic strain on the strain reached at point P_{max}

$$\varepsilon^P = \varepsilon^P(\varepsilon) \tag{6}$$

is shown in Fig. 5. The plastic strain was evaluated for each cycle as the intersection of the cycle tangent (line through points P_{int} and P_{min}) and the strain axis (Fig. 2). The strain values ε are the strains at the P_{max} points, where unloading for each cycle begins. The point for the unloaded state $[\varepsilon, \varepsilon^P] = [0, 0]$ was added and the function was resampled with the same frequency as the envelope curves (Fig. 3). The damage behavior is also noticeable from the dependency of plastic strain on maximum reached strain. The dependency $\varepsilon^p(\varepsilon)$ is shown in Fig. 5. The ability to undergo large plastic deformation (plastic strain ε^p) increases with increasing curing time.

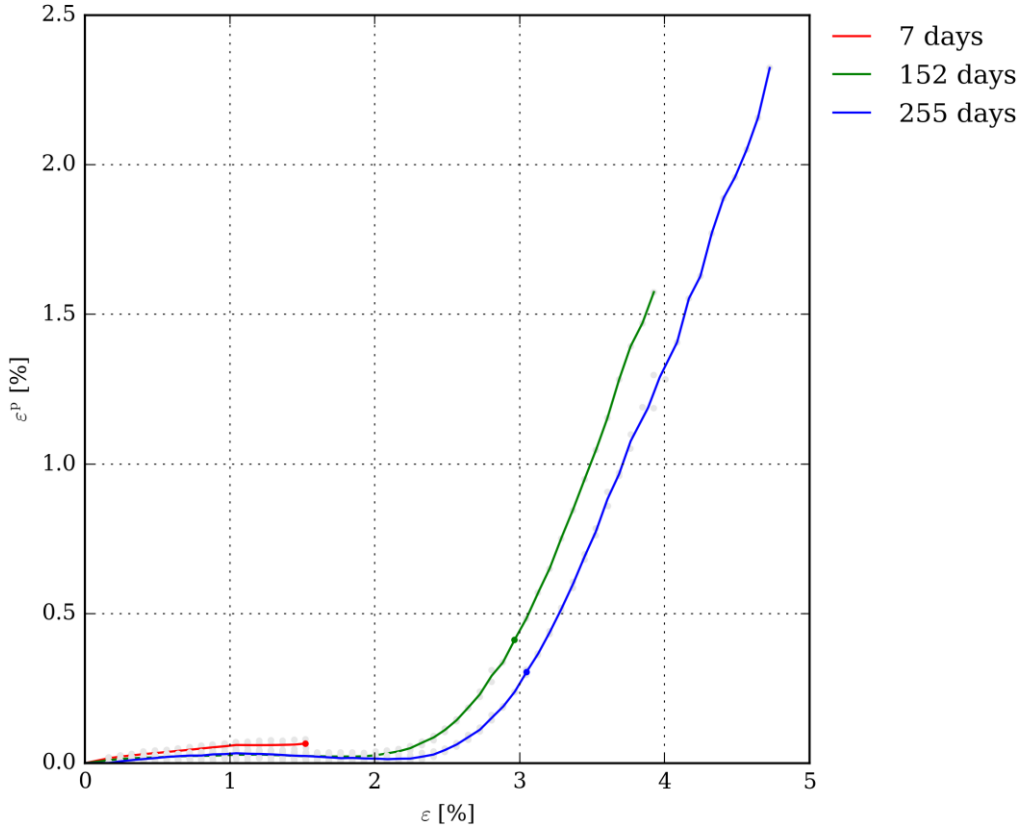

Figure 5: Plastic strain-strain dependencies, points of the highest reached stress σ_{max}.

The specimens cured for 7 days cracked by brittle fracture. On the other hand, the specimens cured for 152 and 255 days withstood loading cycles even after reaching the highest stress σ_{max}.

Damage functions in form of dependency of the damage factor on strain $D(\varepsilon)$ or elastic strain $D(\varepsilon^e)$ are shown in (Fig. 6). The graphs show that the damage function in case of material which is not failed at the maximum reached stress is desirable to be described in the form $D(\varepsilon)$. Damage function in form of $D(\varepsilon^e)$ for the first set of experiments with a different definition of the damage factor D is presented in [3].

The damage associated energy is a function describing the damage evolution in the material. It is defined by integral of the effective stress (3) as

$$B(\varepsilon) = \int_0^{\varepsilon} \bar{\sigma}(\epsilon) \mathrm{d}\epsilon. \tag{7}$$

By expressing the damage evolution dependency B on the damage factor D as

$$B = B(D), \tag{8}$$

a dependency used for material model in *Abaqus CAE* is obtained (Fig. 7).

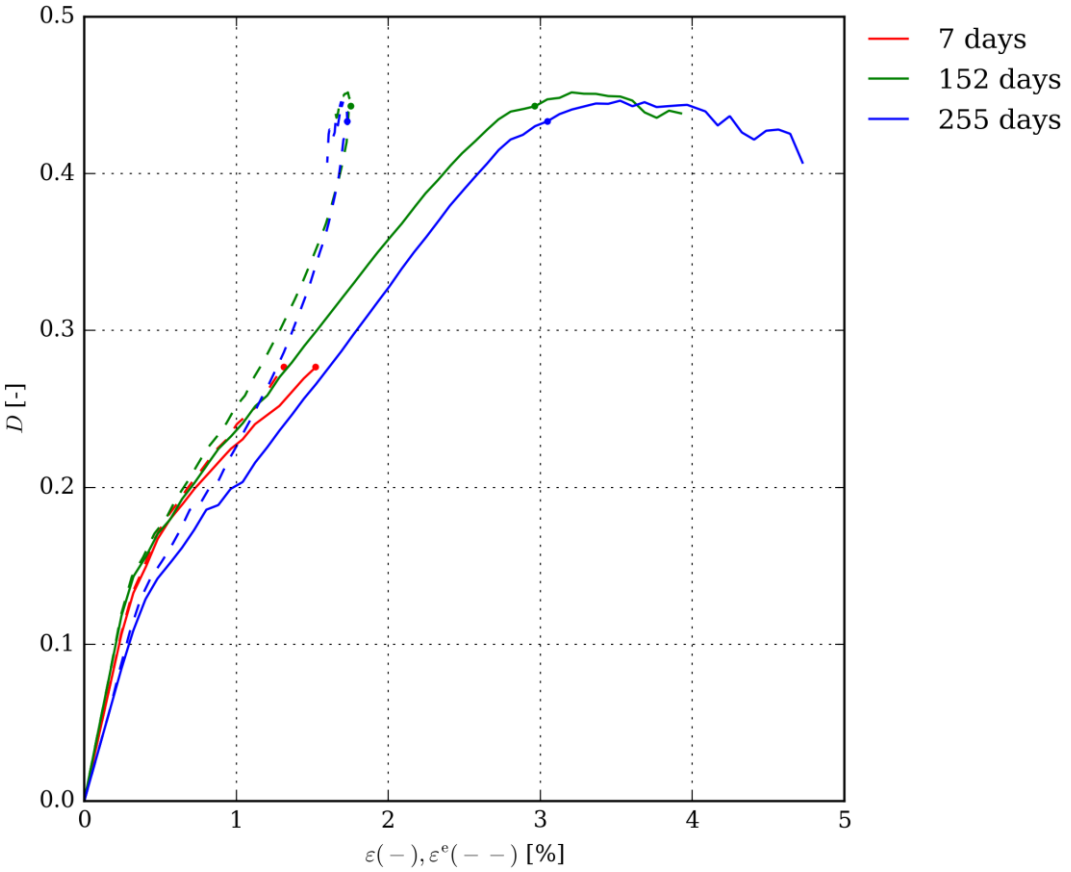

Figure 6: Damage factor-strain and damage factor-elastic strain dependencies, points of the highest reached stress σ_{max}.

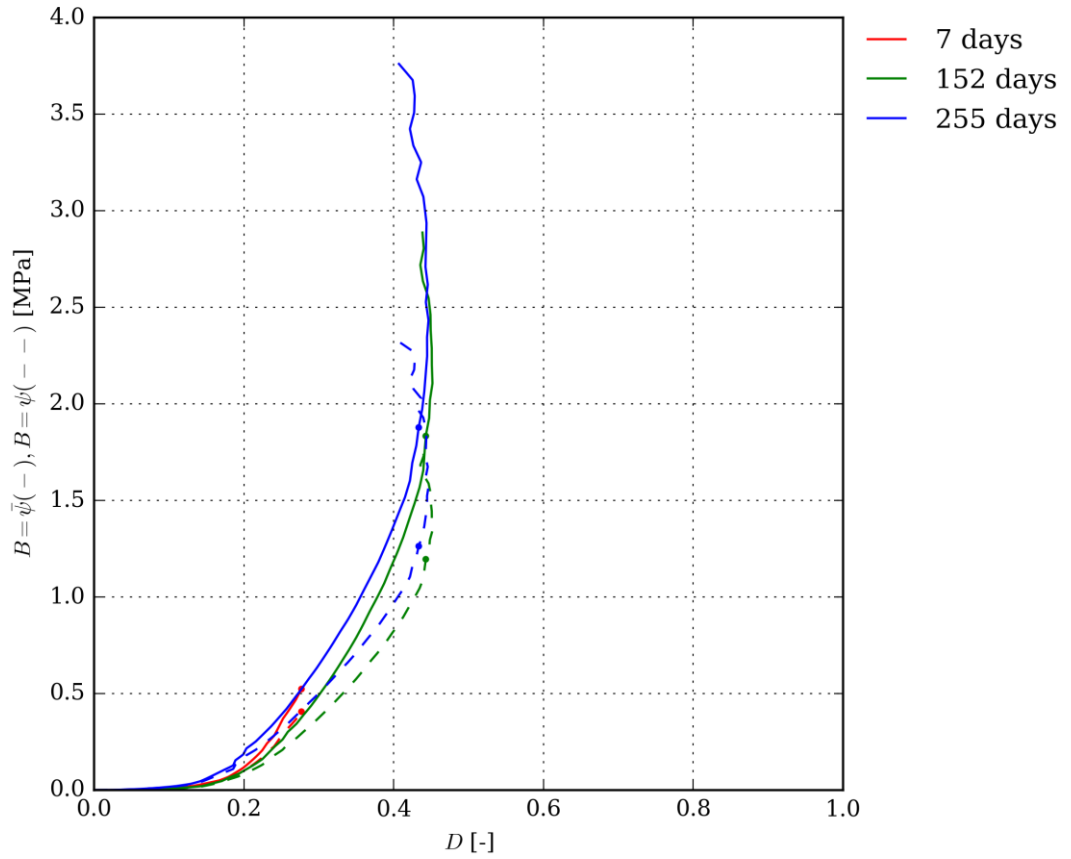

Figure 7: Damage evolution energy-damage factor dependency.

The dependency of damage evolution energy on damage factor shows that the epoxy resin with the shortest time of curing can absorb the lowest amount of damage energy (Fig. 7). The epoxy cured for 7 days is the most brittle material. The parts of the dependencies, where the value of the damage factor has two or more values of the energy are removed before assigning to the material model.

Next material characteristic for material model with plastic behavior is hardening curve displayed in Fig. 9. Hardening curve is a yield stress function of equivalent plastic strain $R = R(\bar{\varepsilon}^{\mathrm{p}})$. For material model considering damage behavior it is also advantageous to define dependency (Fig. 9)

$$\bar{R} = \bar{R}(\bar{\varepsilon}^{\mathrm{p}}), \tag{9}$$

where for a uniaxial stress $\bar{R}$ is equivalent stress $\bar{\sigma}$ and the equivalent plastic strain is equal to the plastic strain $\varepsilon^{\mathrm{p}} \equiv \bar{\varepsilon}^{\mathrm{p}}$.

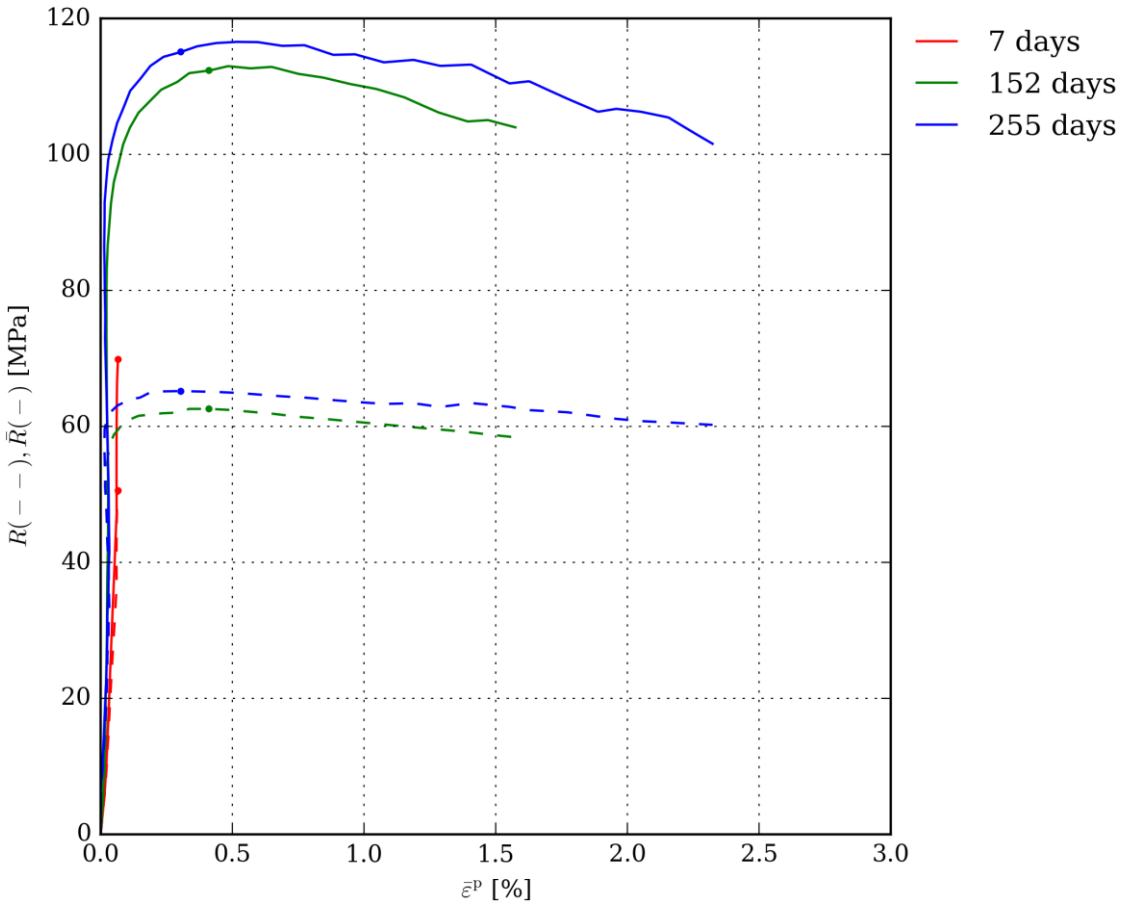

Figure 9: Equivalent stress-equivalent plastic strain dependency and yield stress-equivalent plastic strain dependency (hardening curve).

The parasitic effect seen in Fig. 5 where the plastic strain is not monotonically increasing function of maximum reached strain has the consequence that the equivalent plastic strain is not an increasing function (Fig. 9). This experimentally obtained error should be avoided in correct material model.

Conclusions

Library of functions for processing experimentally obtained data was created. It was used for obtaining crucial parameters from three sets of experiments on epoxy resin. The effect of curing time of epoxy resin was expressed by evaluating material parameters averaged within the sets as well as by depicting the averaged stress strain dependencies.

The tool built in the work enables to process a large number of experiments and visualize them in terms of various dependencies. Sets of data may be averaged in different sets according to the user defined aspect. The data may be either expressed graphically or numerically. The proposed library also enables the user to save the experimental and processed data in a structured data file with all desired information. A structure system exploiting data type with keys designating all the saved data was proposed for the structure of the data organization. This system enables synoptical data sorting and clear storage system.

The processed data may be further used in finite element software. The dependencies may be used in finite element software either to define material properties or in identification processes (e.g. material model calibration). Data from the cyclic tensile tests of the epoxy resin will be further used for defining material models of a substituent (matrix) of carbon/epoxy long-fiber composite materials.

In further authors' work, the cyclic tensile tests will be performed on specimens made of thermoplastic material. The value of the reloading force (stress) at point P_{min} will be set a constant in next author's work. The recently defined increasing value of the start of the loading process causes inaccuracies in further data processing.

Elasto-plastic material model with damage proposed in [3] will be validated with the experimental data processed by the proposed approach with use of the library of functions *ploTRA*.

Acknowledgement

This publication was supported by the project LO1506 of the Czech Ministry of Education, Youth and Sports.

References

[1] ASTM D638-10, Standard Test Method for Tensile Properties of Plastics, ASTM International, 2010.

[2] ISO 527-1, Plastics – determination of tensile properties part 1: General principles. International Organization for Standardization, Geneva, Switzerland, 2012.

[3] Kroupa, T., Srbová, H., Klesa, J. One-Dimensional Elasto-plastic Material Model with Damage for Quick Identification of Material Properties. Materials and Technology, 51(2), 2017. ISSN 1580-2949.